COBEM 2021 26th International Congress of Mechanical Engineering
November 22-26, 2021, Virtual Congress, Brazil
ABCM Associação Brasileira de Engenharia e Ciências Mecânicas

COB-2021-1399
A FINITE ELEMENT METHOD ANALYSIS FOR THE INTERLAMINAR FAILURE MODELLING OF THIN SYMMETRIC LAMINATED COMPOSITE PLATES

Armando Italo de Paula Gonçalves
Carlos Henrique Daros
Faculdade de Engenharia Mecânica da Universidade Estadual de Campinas - FEM/UNICAMP Rua Mendeleyev, 200 - CEP 13083-860, Cidade Universitária "Zeferino Vaz" Barão Geraldo, Campinas - SP
a213243@dac.unicamp.br; chdaros@fem.unicamp.br

Abstract. *A linear finite element analysis is considered here for the static modelling of thin symmetric laminated composite plates. Composite laminates are applied in various engineering fields, e.g., in aerospace structures. The Classical Plate Theory (CPT) for Laminates is the equivalent of Kirchhoff's Theory for simple plates. The kinematic assumptions of Kirchhoff's Theory allow an excellent modelling of thin plates. However, the CPT does not include the out-of-plane stress state, which is vital for assessing the interlaminar stresses on laminated composite plates. But integration of the equilibrium equations in strong form allows the recovery of the out-of-plane stress state, provided the finite element has a sufficient degree of continuity. Hence, by recovering the interlaminar stresses we may use some available failure criteria for the interlaminar failure of laminated composites. We shall examine one type of polynomial approximation for finite elements for plates to recover the out-of-plane stress state, aiming at studying the interlaminar failure of laminated composites via the modified Tsai-Wu failure criteria.*

Keywords: *interlaminar failure, finite element method, laminated composites*

1. INTRODUCTION

Several of the current engineering projects require material properties that are only achieved by using composite materials, for example orthotropic unidirectional fiber-reinforced laminates. The laminated composites are made up by laying various unidirectional fiber-reinforced laminae with different properties and orientations.

This paper proposes a method using a linear finite element analysis and the Classical Plate Theory (CPT) to calculate the displacement and interlaminar stress of thin symmetric laminated composite plates. Since the present formulation is restricted for thin plates, it does not contain the shear energy as in the Reisner-Mindlin plates, where, due to reduced integration, the spurious energy modes may be presented. In addition, the study will be extended to a interlaminar stress failure investigation that will be developed based on the modified Tsai-Wu criterion present in Naik, Gillespie, and Eduljee (2019).

In order to obtain the interlaminar stress fields, such as the normal stress σ_{zz}, it is necessary at least an approximated displacement field with C4 continuity. Higher order triangular finite elements for plate bending problems can be found in, e.g., TUBA family (Argyris, Fried, and Scharpf, 1968) of elements and the refined triangular elements (Bell, 1969). For rectangular finite elements (Bogner, Fox, Schmit, 1966) derived Higher order Hermite Polynomial elements which have six (P6) and nine (P9) degrees of freedom per node, finite elements possessing C5 continuity. However, those elements can be complex to implement, since they use higher order derivatives as curvatures. As an alternative method, the present work uses the P4 element, also described in Bogner, Fox, and Schmit (1966), that uses third-order Hermite polynomials, which, despite having C3 continuity, has excellent convergence. The Finite Difference Method (FDM) can be implemented, as part of the post-processing, with the aim of supplementing the lack of continuity of the stress field derivatives which will be necessary to obtain the interlaminar stresses of the plate.

2. FORMULATION

2.1 Governing Equations

We will consider the bending of thin symmetrically laminated plates. Consequently, according to Reddy (2004) "the equations for bending deflection are uncoupled from those of the stretching displacements. If the in-plane forces are zero, the in-plane displacements (u, v) are zero, and the problem is reduced to one of solving for bending deflection and stresses". Thus the governing equations to the kth layer is obtained using the generalized Hooke's Law and it is given by

Reddy (2004):

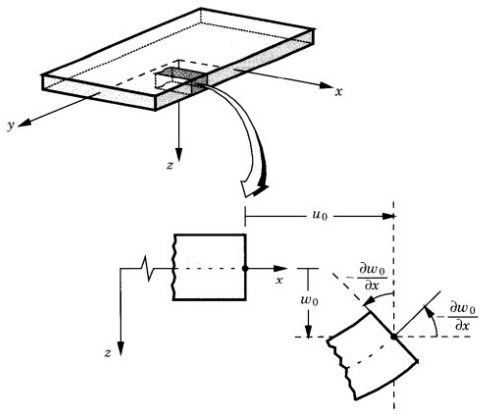

Figure 1. Kirchhoff's plate kinematics, where (u_0,w_0) are the (x,z) displacements of the midplane point. Image taken from Reddy (2004).

$$\begin{Bmatrix} \epsilon_{xx} \\ \epsilon_{yy} \\ \epsilon_{xy} \end{Bmatrix} = \begin{Bmatrix} -\frac{\partial^2 w}{\partial x^2} \\ -\frac{\partial^2 w}{\partial y^2} \\ -2\frac{\partial^2 w}{\partial y \partial x} \end{Bmatrix}, \tag{1}$$

$$\begin{Bmatrix} \sigma_{xx} \\ \sigma_{yy} \\ \tau_{xy} \end{Bmatrix} = z \begin{bmatrix} \overline{Q}_{11} & \overline{Q}_{12} & \overline{Q}_{16} \\ \overline{Q}_{12} & \overline{Q}_{22} & \overline{Q}_{26} \\ \overline{Q}_{16} & \overline{Q}_{26} & \overline{Q}_{66} \end{bmatrix} \begin{Bmatrix} -\frac{\partial^2 w}{\partial x^2} \\ -\frac{\partial^2 w}{\partial y^2} \\ -2\frac{\partial^2 w}{\partial y \partial x} \end{Bmatrix}, \tag{2}$$

$$\begin{Bmatrix} M_{xx} \\ M_{yy} \\ M_{xy} \end{Bmatrix} = \begin{bmatrix} D_{11} & D_{12} & D_{16} \\ D_{12} & D_{22} & D_{26} \\ D_{16} & D_{26} & D_{66} \end{bmatrix} \begin{Bmatrix} -\frac{\partial^2 w}{\partial x^2} \\ -\frac{\partial^2 w}{\partial y^2} \\ -2\frac{\partial^2 w}{\partial y \partial x} \end{Bmatrix}, \tag{3}$$

$$\overline{Q}_{11} = Q_{11}\cos^4(\phi) + 2(Q_{12} + 2Q_{66})\sin^2(\phi)\cos^2(\phi) + Q_{22}\sin^4(\phi), \tag{4}$$

$$\overline{Q}_{12} = (Q_{11} + Q_{22} - 4Q_{66})\sin^2(\phi)\cos^2(\phi) + Q_{12}(\sin^4(\phi) + \cos^4(\phi), \tag{5}$$

$$\overline{Q}_{22} = Q_{11}\sin^4(\phi) + 2(Q_{12} + 2Q_{66})\sin^2(\phi)\cos^2(\phi) + Q_{22}\cos^4(\phi), \tag{6}$$

$$\overline{Q}_{16} = (Q_{11} - Q_{12} - 2Q_{66})\sin(\phi)\cos^3(\phi) + (Q_{12} - Q_{22} + 2Q_{22})\sin^3(\phi)\cos(\phi), \tag{7}$$

$$\overline{Q}_{26} = (Q_{11} - Q_{12} - 2Q_{66})\sin^3(\phi)\cos(\phi) + (Q_{12} - Q_{22} + 2Q_{22})\sin(\phi)\cos^3(\phi), \tag{8}$$

$$\overline{Q}_{66} = (Q_{11} + Q_{22} - 2Q_{12} - 2Q_{66})\sin^2(\phi)\cos^2(\phi) + Q_{66}(\sin^4(\phi) + \cos^4(\phi)), \tag{9}$$

$$Q_{11} = \frac{E_{11}}{1 - \upsilon_{12}\upsilon_{21}}, \qquad Q_{12} = \frac{\upsilon_{12}E_{11}}{1 - \upsilon_{12}\upsilon_{21}}, \qquad Q_{22} = \frac{E_{22}}{1 - \upsilon_{12}\upsilon_{21}}, \qquad Q_{66} = G_{12}, \tag{10}$$

$$D_{ij} = \frac{1}{3}\sum_{k=1}^{N} \overline{Q}_{ij}^{(k)}(z_{k+1}^3 - z_k^3). \tag{11}$$

Where, w is the transverse displacement, ϵ is the strain, σ is the normal stress, τ is the shear stress, M is the bending moment, ϕ represents the laminate's fiber orientation, E is the elastic modulus, υ is the Poisson's ratio, and G is the shear modulus.

The assumption present in CPT yields constitutive equations in which the interlaminar stresses τ_{xz}, τ_{yz}, and σ_{zz} are zero. However, in most cases, these stresses can not be neglected, and in some cases, they can be responsible for the plate failure. Therefore, these stresses are obtained by integrating the equilibrium equations of 3-D elasticity and according to (Patton *et al.*, 2021), they are given:

$$\tau_{xz}(z) = -\int_{\bar{z}}^{z} (\sigma_{x,x}(\zeta) + \tau_{xy,y}(\zeta))d\zeta + \tau_{xz}(\bar{z}), \tag{12}$$

$$\tau_{yz}(z) = -\int_{\bar{z}}^{z} (\tau_{xy,x}(\zeta) + \sigma_{y,y}(\zeta))d\zeta + \tau_{yz}(\bar{z}), \tag{13}$$

$$\sigma_{zz}(z) = \int_{\bar{z}}^{z} \left[\int_{\bar{z}}^{\zeta} (\sigma_{x,xx}(\xi) + \sigma_{y,yy}(\xi) + 2\tau_{xy,xy}(\xi))d\xi \right] d\zeta - (z-\bar{z})(\tau_{xz,x}(\bar{z}) + \tau_{yz,y}(\bar{z})) + \sigma_{zz}(\bar{z}). \tag{14}$$

"Where ζ represents the coordenate along the plate thickness direction, and the integral constants should be chosen to fulfill the boundary conditions at the top or bottom surfaces $\bar{z}$".

2.2 Analytical solution

In this subsection an analytical solutionn will be used to compare the results obtained by proposed the numerical algorithm. This method, known as Navier solution, is used to analytically solve all four edges of simply supported orthotropic plates. The procedure consists in expanding the transverse deflection $w(x, y)$ and the load $q(x, y)$ in double Fourier series and satisfying the simply supported plate boundary conditions.

For a rectangular plate whose length along x direction is a, length along y direction is b, the simply supported conditions composed by zero transverse deflection at the edges and the bending moments $M_{xx}(0, y)$, $M_{xx}(a, y)$, $M_{yy}(x, 0)$, $M_{yy}(x, b)$. Therefore the analytical equations are given as follows Reddy (2004):

$$w(x,y) = \sum_{m=1}^{\infty}\sum_{n=1}^{\infty} W_{mn} \sin\left(\frac{m\pi x}{a}\right) \sin\left(\frac{n\pi y}{b}\right), \tag{15}$$

$$W_{mn} = \frac{Q_{mn}}{\frac{1}{b^4}\pi^4(D_{11}m^4(\frac{b}{a})^4 + 2m^2n^2(\frac{b}{a})^2(D_{12}+2D_{66}) + D_{22}n^4)}. \tag{16}$$

For uniformly distributed load q_0 and for odd m and n:

$$Q_{mn} = \frac{16q0}{\pi^2 mn}. \tag{17}$$

2.3 Finite Element Formulation

In order to obtain the weak form associated with the orthotropic plate, the principle of virtual work will be used. The principle requires that the variation of the strain energy and the variation of external work are equal. For these conditions, the strain energy (U) for the actual strains and the external work (V) produced by a uniformly distributed load q_0 acting in the rectangular plate are given by Shames, and Dym (1985):

$$U = \int_V (\epsilon_{xx}\sigma_{xx} + \epsilon_{yy}\sigma_{yy} + 2\epsilon_{xy}\sigma_{xy})dV, \tag{18}$$

$$V = \int\int_A q_0 w(x,y)dA. \tag{19}$$

The first integral with respect to z integration of Eq. (18) yields:

$$U = \int\int_A \left(M_{xx}\frac{\partial^2 w}{\partial x^2} + M_{yy}\frac{\partial^2 w}{\partial y^2} + M_{xy}\frac{\partial^2 w}{\partial y \partial y} \right) dA. \tag{20}$$

From Eq. (3) and Eq. (21) and principle of virtual work:

$$\int\int_A (\{\delta\epsilon\}^T\{M\} - q_0\delta w(x,y))dA. \tag{21}$$

In this section a vector of interpolating functions $[N]$, is used to describe the transverse deflection field $w(x, y)$ in function of the nodal displacements matrix a. In addition, we will use the operator L defined by $L[w(x, y)] = \{\epsilon\}$ and Eq. (21) in Eq. (3) to obtain:

$$[K]^e \{a\}^e = \{q\}^e, \tag{22}$$

With:

$$[K]^e = \int\int_A [L(N)]^T [D][L(N)]dA, \tag{23}$$

and:

$$\{q\}^e = \int\int_A [N]q_0 dA. \tag{24}$$

2.4 P4 Element

According to Zienkiewicz *et al.* (2013), the P4 Element is the rectangular element that has the best convergence and it satisfies the patch tests of rigid body motion and constant strain state. The element has four nodal points, with four possible nodal displacements (w, $\frac{\partial w}{\partial x}$, $\frac{\partial w}{\partial y}$, $\frac{\partial^2 w}{\partial x \partial x}$) each, located at the corners. The P4 is a conforming element, which possesses compatibility of displacement and rotation between its edges, and makes use of the third-order Hermite polynomials to interpolate the transverse deflection inside the element's domain. These Hermite polynomials for the P4 element and their derivatives can be given by Bogner, Fox, and Schmit (1966):

$$H_{01}^{1\gamma} = \frac{1}{a_\gamma^3}(2x_\gamma^3 - 3a_\gamma x_\gamma^2 + a_\gamma^3), \tag{25}$$

$$H_{02}^{1\gamma} = -\frac{1}{a_\gamma^3}(2x_\gamma^3 - 3a_\gamma x_\gamma^2), \tag{26}$$

$$H_{11}^{1\gamma} = -\frac{1}{a_\gamma^2}(x_\gamma^3 - 2a_\gamma x_\gamma^2 + a_\gamma^2), \tag{27}$$

$$H_{12}^{1\gamma} = -\frac{1}{a_\gamma^2}(x_\gamma^3 - a_\gamma x_\gamma^2). \tag{28}$$

With $\gamma = 1, 2$ and a_1, a_2 are the finite element dimensions in the x and y local coordinates, respectively.

Thus, the shape function vector to the ij node is:

$$H_{ij} = \{H_{0i}^{11} H_{0j}^{12}, H_{1i}^{11} H_{0j}^{12}, H_{0i}^{11} H_{1j}^{12}, H_{1i}^{11} H_{1j}^{12}\}^T, \tag{29}$$

and the vector of interpolating functions $[N]$ is given by:

$$[N] = \{H_{11}, H_{21}, H_{22}, H_{21}\}^T. \tag{30}$$

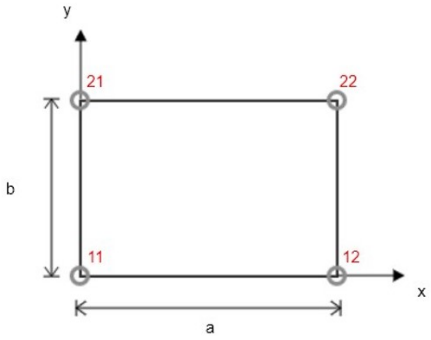

Figure 2. ij nodes in a element.

2.5 Finite Difference Formulation

The computation of the interlaminar stress σ_{zz} requires the fourth derivative of the approximate deflection field. Since the P4 element does not possess continuity for higher order derivatives (e.g., $\frac{\partial^2 w}{\partial x^2}$) between the elements, their values will be evaluated at the centroid of each finite element. The centroidal values will be the used to obtain the fourth order derivatives via the FDM, as follows:

$$\frac{\partial w^4(x_c, y_c)}{\partial x^4} = \frac{\frac{\partial w^2(x_c+\Delta x, y_c)}{\partial x^2} - 2\frac{\partial w^2(x_c, y_c)}{\partial x^2} + \frac{\partial w^2(x_c-\Delta x, y_c)}{\partial x^2}}{\Delta x^2}, \tag{31}$$

$$\frac{\partial w^4(x_c, y_c)}{\partial y^4} = \frac{\frac{\partial w^2(x_c, y_c+\Delta y)}{\partial y^2} - 2\frac{\partial w^2(x_c, y_c)}{\partial y^2} + \frac{\partial w^2(x_c, y_c-\Delta y)}{\partial y^2}}{\Delta y^2}. \tag{32}$$

With (x_c, y_c) is the element centroid coordinate, $\Delta x = a$, and $\Delta y = b$.

2.6 Modified Tsai-Wu Failure Criteria

Once the stress field has been obtained, a failure analysis can be further pursued. The Modified Tsai-Wu Failure Criteria for fiber-matrix will be used, which assumes that only interlaminar stresses between the fibers and the composites matrix interact to influence interlaminar failure and the in-plane stresses have a negligible influence on interlaminar failure. Thus, using these assumptions, according to Naik, Gillespie and Eduljee (2019), the Tsai-Wu polynomial is simplified to:

$$F_3\sigma_{zz} + F_{33}\sigma_{zz}^2 + F_{44}\tau_{yz}^2 + F_{55}\tau_{xz}^2 = 1, \tag{33}$$

With,

$$F_3 = \frac{1}{S_{zzt}} + \frac{1}{S_{zzc}}, \qquad F_{33} = \frac{-1}{S_{zzt}S_{zzc}}, \qquad F_{44} = \frac{1}{S_{yz}^2}, \qquad F_{55} = \frac{1}{S_{xz}^2}. \tag{34}$$

and S_{zzt} is the interlaminar tension strength, S_{zzc} is the interlaminar compression strength, S_{yz} is the interlaminar (or transverse) shear strength in the yz-plane, and S_{xz} is the interlaminar shear strength in the xz-plane of the composite.

3. RESULTS

In the next section, the results of two practical applications are shown. Both analysis focus on the use of a Carbon-Epoxy composite plate, with square shape 2x2 meters, 0.03 m of thickness, three symmetrical layers ($h = 0.01$ m for each), and engineering properties showed in Tab. 1, under uniformly distributed load $q_0 = 2$ MPa. The first one is a symmetric simply supported plate, which has the stress field compared with the Navier analytical solution. The second one is an asymmetric clamped plate, which has the transverse displacement compared with the solution obtained by the software Abaqus. The finite element type used in the Abaqus environment was the TRI3 element that according to the Abaqus Theory Manual, "imposes the Kirchhoff constraint analytically".

Table 1. Carbon-Epoxy composite properties.

E_x, GPa	E_y, GPa	G_{xy}, GPa	ν_{xy}	S_{zzt}, MPa	S_{zzc}, MPa	S_{yz}, MPa	S_{xz}, MPa
139.2	8.076	5.00	0.324	25.0	−834.3	62.1	62.1

Since the domain of the laminated plate problem under discussion is symmetrical, in order to achieve faster convergence, just one-quarter of the domain (fourth quadrant) is divided into elements and solved. Thus, the finite elements are distributed only in this quadrant in a 9x9 mesh with 81 elements, as can be seen in Fig. 3.

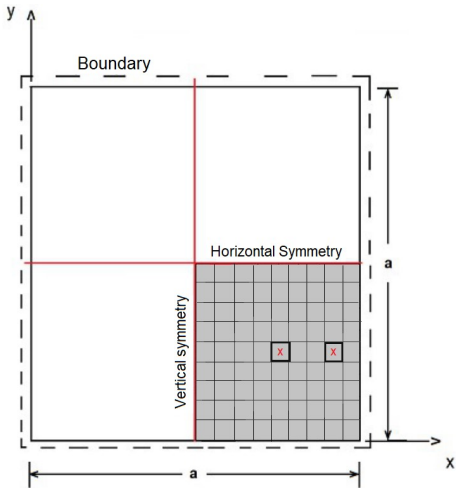

Figure 3. points of interest at the centroid of the highlighted elements, the mesh's domain and its boundary scheme, where the dashed line represents boundary and the red line the symmetry lines.

3.1 Orthotropic Simply Supported Plate

The fiber orientation per layer is given by $\phi = [0°, 90°, 0°]$, that is an orthotropic plate. In addition, the boundary conditions for simply supportedplate are $w = \frac{\partial w}{\partial x} = 0$ for the bottom edge and $w = \frac{\partial w}{\partial y} = 0$ for the right one, besides, the one-quarter symmetry gives that $\frac{\partial w}{\partial x} = 0$ on the vertical symmetry line and $\frac{\partial w}{\partial y} = 0$ on the horizontal symmetry line.

In order to validate the algorithm, the numerically calculated interlaminar stress σ_{zz} , τ_{xz} and τ_{yz} along the thickness are compared analytically calculated in some points of interest, as the center of the mesh's domain $(1.5; 0.5)$ and the point near the edge $(1.83; 0.5)$, whose significance will be examined later. Both points are marked in Fig. 3. The high similarity between the results obtained, can be checked in Fig. 4, 5, 6, 7, 8, and 9, where the different colors represent each plate's layer.

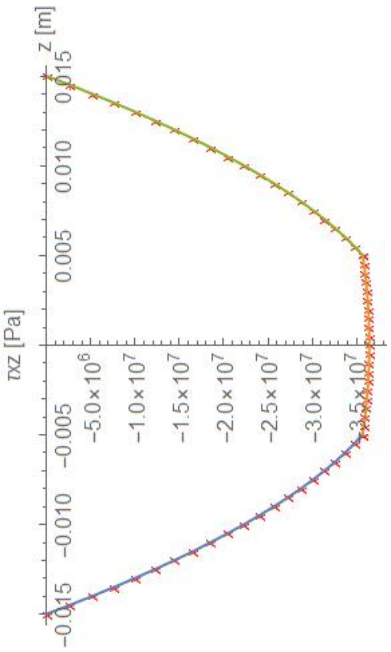

Figure 4. Numerical solution in "x" marker and analytical solution in continuous line for τ_{xz} at $(1.5; 0.5)$.

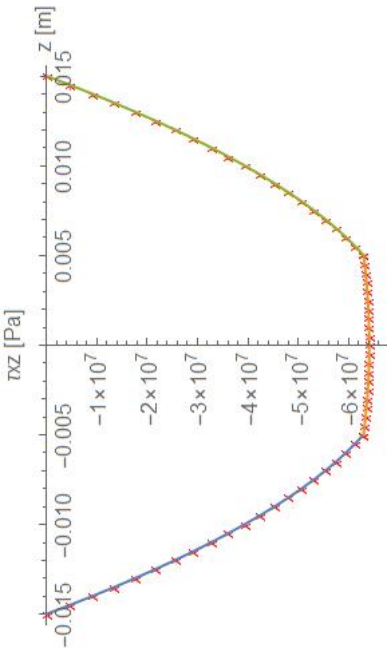

Figure 5. Numerical solution in "x" marker and analytical solution in continuous line for τ_{xz} at $(1.83; 0.5)$.

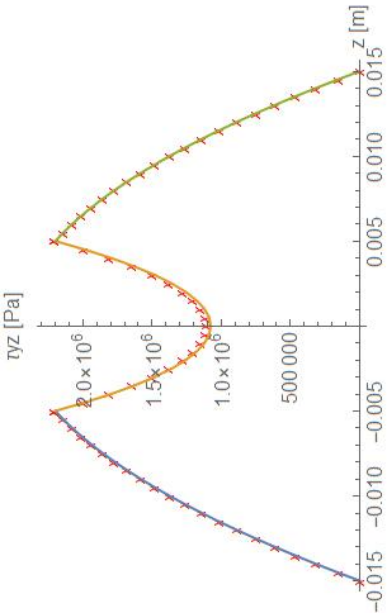

Figure 6. Numerical solution in "x" marker and analytical solution in continuous line for τ_{yz} at $(1.5; 0.5)$.

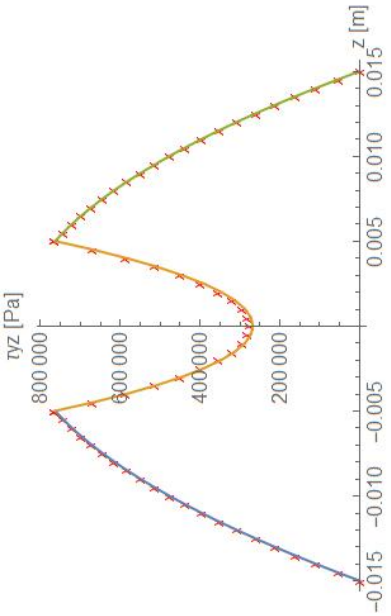

Figure 7. Numerical solution in "x" marker and analytical solution in continuous line for τ_{yz} at $(1.83; 0.5)$.

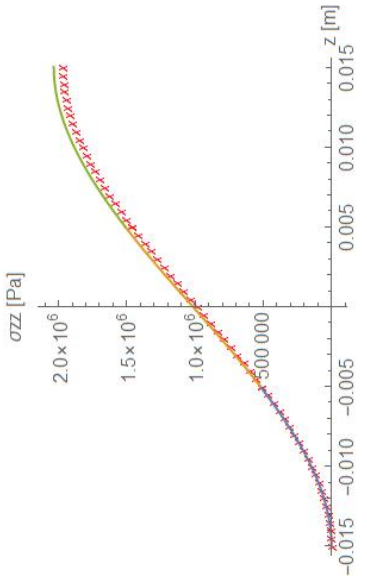

Figure 8. Numerical solution in "x" marker and analytical solution in continuous line for σ_{zz} at $(1.5; 0.5)$.

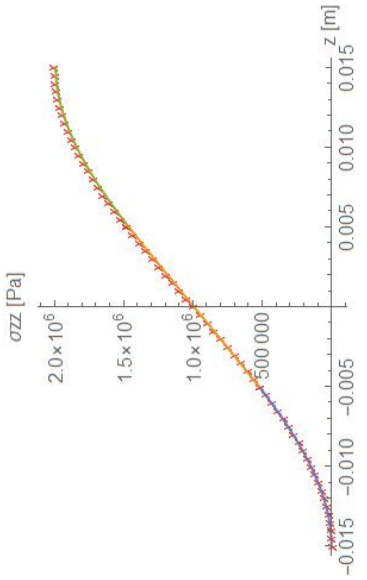

Figure 9. Numerical solution in "x" marker and analytical solution in continuous line for σ_{zz} at $(1.83; 0.5)$.

In the Finite Element Method, convergence is a serious issue, mostly near the boundary, thus, an analysis of this parameter is extremely important to the present work. Therefore, the result obtained by using a less dense mesh (3x3) are compared to the results by using the 9x9 mesh previously presented, for $z = 0$, at the points of interest, which have the notoriety of being the centroid of elements of different meshes.

Table 2. Results for different meshes for points A = $(1.5; 0.5)$ and B = $(1.83; 0.5)$.

	Point	w (m)	τ_{xz} (Pa)	τ_{yz} (Pa)	σ_{zz} (Pa)
3x3 Mesh	A	0.711	$-3.64\ 10^7$	$9.91\ 10^5$	$9.91\ 10^5$
9x9 Mesh	A	0.711	$-3.64\ 10^7$	$1.11\ 10^6$	$9.86\ 10^5$
Analytical	A	0.711	$-3.64\ 10^7$	$1.08\ 10^6$	$9.92\ 10^5$
3x3 Mesh	B	0.263	$-6.41\ 10^7$	$3.82\ 10^5$	$1.00\ 10^6$
9x9 Mesh	B	0.263	$-6.41\ 10^7$	$2.79\ 10^5$	$1.00\ 10^6$
Analytical	B	0.263	$-6.41\ 10^7$	$2.68\ 10^5$	$1.00\ 10^6$

Table 2 shows that w, τ_{xz}, and σ_{zz} have fast convergence, showing accuracy even for a low-density mesh, even near the boundary, besides that, the 9x9 mesh gives a result really close to the analytical. Thus, it is concluded that the presented algorithm has good convergence.

Once validated the interlaminar stress field obtained via the program, the next post-processing step is to apply the Modified Tsai-Wu failure criteria, presented in Eq.(33). The failure analysis is assessed for each element's centroid, evaluating the maximum equation's value in each layer. After that, the values are separated by lamina, and a color map is drawn for all layers. Figure 10 shows the result for the plate's middle layer, which is the most critical one.

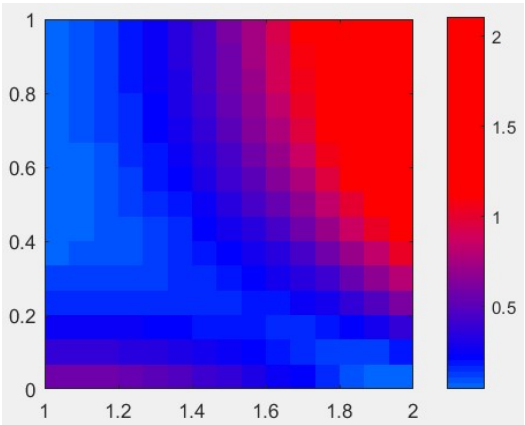

Figure 10. Modified Tsai-Wu failure criteria result for the middle layer at the fourth quadrant of the plate.

3.2 Anisotropic Clamped Plate

The Abaqus software has been used here to validate the results of this section since there is no analytical solution for the monoclinic square plate with all edges clamped. However, the finite element type used to reproduce the Kirchhoff's constraints does not give the interlaminar stress, so just the transverse displacement will be compared (Fig. 11). For this study, the fiber orientation per layer is given by $\phi = [0°, 30°, 0°]$, that is an anisotropic plate. The boundary conditions for the clamped case are: $w = \frac{\partial w}{\partial x} = \frac{\partial w}{\partial y} = \frac{\partial^2 w}{\partial x \partial y} = 0$ for the bottom and right edges, the symmetry ones are the same: $\frac{\partial w}{\partial x} = 0$ and $\frac{\partial w}{\partial y} = 0$ on the vertical and horizontal symmetry lines, respectively.

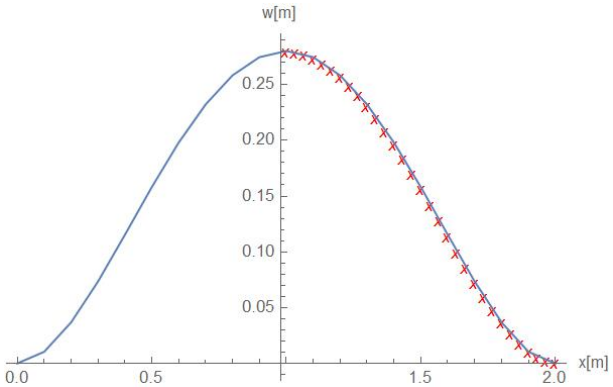

Figure 11. Numerical solution in red "x" marker and Abaqus solution in blue continuous line for $w(x, y)$ at the horizontal symmetrical line $y = 1m$.

Analogous to the former case, the interlaminar stress τ_{xz}, τ_{yz}, and σ_{zz} are calculated by the numerical method and used in the Modified Tsai-Wu failure analysis, the results shown in Fig. 12, 13, 14, and 15 respectively, where the chosen layer was the middle one, which is the most critical. Although no analytical solution is available here, neither does the software Abaqus furnishes the out-of-the plane stresses for the STRI3 element, the expected results for the stress field, $\sigma_{zz}(z = -\frac{h}{2}) = 0$, $\sigma_{zz}(z = \frac{h}{2}) = q_0$, $\tau_{xz}(z = \pm\frac{h}{2}) = 0$, and $\tau_{yz}(z = \pm\frac{h}{2}) = 0$, are clearly archieved by the numerical results.

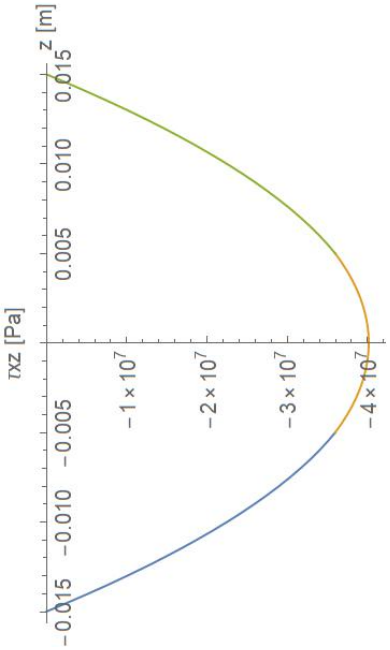

Figure 12. Numerical solution for τ_{xz} at $(1.5; 0.5)$.

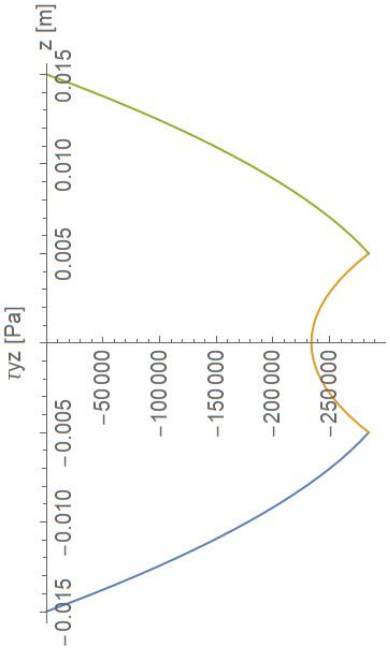

Figure 13. Numerical solution for τ_{yz} at $(1.5; 0.5)$.

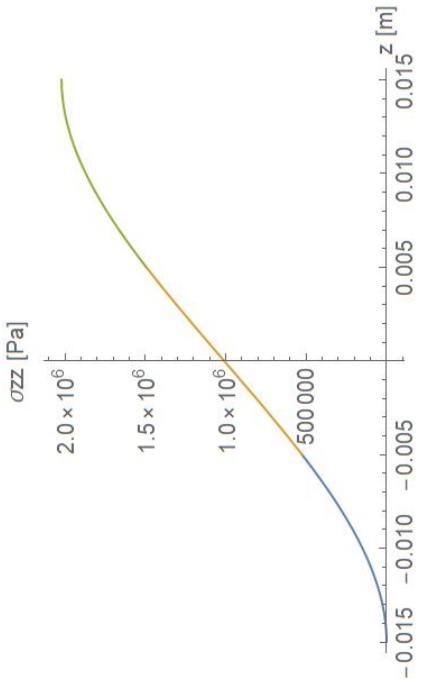

Figure 14. Numerical solution for σ_{zz} at $(1.5; 0.5)$.

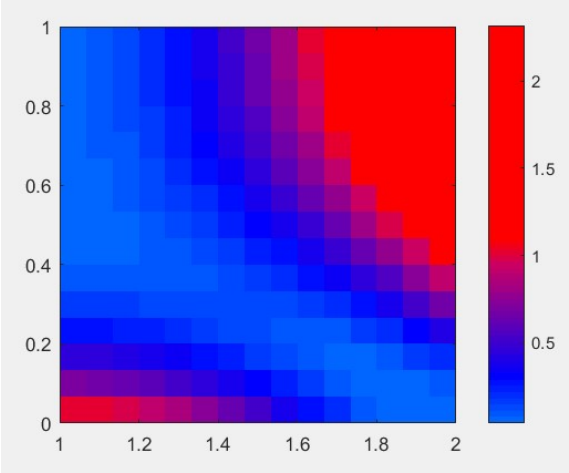

Figure 15. Modified Tsai-Wu failure criteria result for the middle layer at the fourth quadrant of the plate.

3.3 Anisotropic Clamped-Free Plate

Regarding the combinations of different boundaries, the methodology of solving a quarter of the domain is restricted to the horizontal and vertical symmetry conditions, as in Fig 3. However, the method can be extended to any combination, but a higher amount of elements would be required since the problem‘s domain would increase. In this section, the symmetrical clamped-free boundary is explored. The plate is clamped at $y = 0$ and $y = 2$ and free at $x = 0$ and $x = 2$, satisfying the symmetry requirement. As in the last section, the laminated is anisotropic, with fiber orientation per layer is given by $\phi = [90°, 30°, 90°]$. Again, no analytical solution is available, so the same procedure is performed.

The numerical and Abaqus results for transverse displacement are compared in Fig 16 and 17, and in Fig. 18, the Modified Tsai-Wu failure analysis resulted for the plate's middle layer, which is the most critical one.

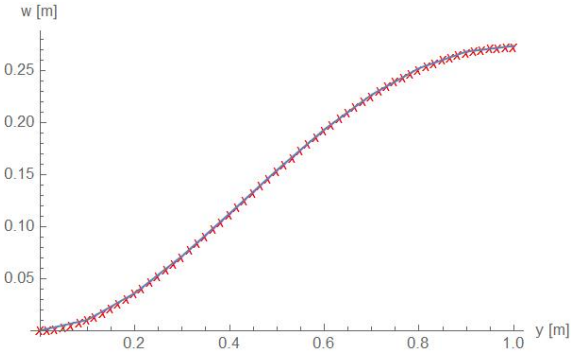

Figure 16. Numerical solution in red "x" marker and Abaqus solution in continuous line for $w(x, y)$ at $x = 1m$.

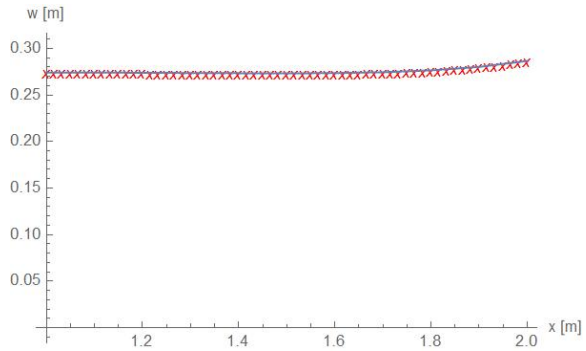

Figure 17. Numerical solution in red "x" marker and Abaqus solution in continuous line for $w(x, y)$ at $y = 1m$.

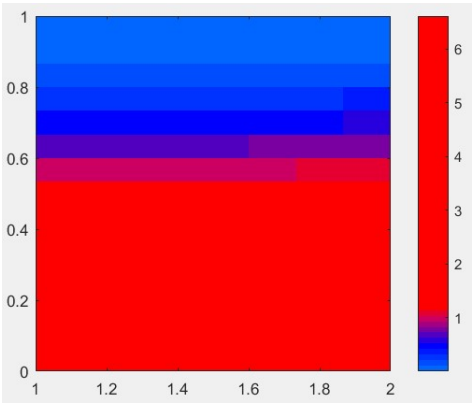

Figure 18. Modified Tsai-Wu failure criteria result for the middle layer at the fourth quadrant of the plate.

4. CONCLUSIONS

The algorithm obtained good results for the transverse displacement and the interlaminar stresses in element centroids located in central region and near the edge. In this sense, the present work introduce a fast convergence program that can be used to evaluate the displacement and interlaminar stresses field of thin symmetric laminated composite plates, besides that, it can indicate the plate interlaminar failure. However, since the program evaluates the stresses at the centroids of the elements only, a dense mesh must be used, in order to estimate the complete stress field, mainly at the edges.

5. REFERENCES

Argyris, J. H., Fried, I., and Scharpf, D. W., 1968. “The TUBA family of plate elements for the matrix displacement method”. *The Aeronautical Journal of the Royal Aeronautical Society*, Vol. 72, p. 701–709.

Bell, K., 1969. “A refined triangular plate bending finite element”. *International Journal for Numerical Methods in Engineering*, Vol. 1, p. 101–122.

Bogner, F. K., Fox, R. L., and Schmit, Jr. L. A., 1966. “The generation of Inter-element-compatible stiffness and mass matrices by the use of interpolation formulas”. In *Matrix Methods in Structural Mechanics*, p. 397-443.

Naik, R. A., Gillespie, JR. J. W., and Eduljee, R. F., 2019. "Development of a modified Tsai-Wu Criterion for Interlaminar Failure in Composite Laminates". *Proceedings of the Eighth Japan-US Conference on Composite Materials*, p. 639-648.

Patton, A. et al.,2021. "Accurate equilibrium-based interlaminar stress recovery for isogeometriclaminated composite Kirchhoff plates". *Composite Structures*, Vol. 256, p. 1-15.

Reddy, J. N., 2004. *Mechanics of Laminated Composite Plates and Shells*. CRC Press, Boca Raton.

Shames, I. H., and Dym, C. L., 1985. *Energy and finite element methods in structural mechanics*.CRC Press, Boca Raton.

Zienkiewicz O. C., Taylor R. L., Nithiarasu P., 2013. *The Finite Element Method for Solid and Structural Mechanics*. Butterworth-Heinemann, Oxford.

6. RESPONSIBILITY NOTICE

The authors are solely responsible for the printed material included in this paper.